

# Structural rearrangements of the two domains of *Azotobacter vinelandii* rhodanese upon sulfane sulfur release: essential molecular dynamics, $^{15}\text{N}$ NMR relaxation and deuterium exchange on the uniformly labeled protein

Daniel Oscar Cicero<sup>a,b</sup>, Sonia Melino<sup>b</sup>, Maria Orsale<sup>b</sup>, Giuseppe Brancato<sup>c</sup>,  
Andrea Amadei<sup>b</sup>, Fabio Forlani<sup>d</sup>, Silvia Pagani<sup>d</sup>, Maurizio Paci<sup>a,b,\*</sup>

<sup>a</sup> INFN, Sez. B, University of Rome Tor Vergata, Rome, Italy

<sup>b</sup> Dipartimento di Scienze e Tecnologie Chimiche, University of Rome "Tor Vergata", Via della Ticerca Scientifica, 00133 Rome, Italy

<sup>c</sup> Dipartimento di Chimica, University of Rome "La Sapienza", Rome, Italy

<sup>d</sup> Dipartimento di Scienze Molecolari Agroalimentari, University of Milano, Milan, Italy

Received 9 May 2003; received in revised form 1 August 2003; accepted 6 August 2003

## Abstract

The *Azotobacter vinelandii* rhodanese is a 31 kDa sulfurtransferase protein that catalyzes the transfer of sulfur atom from thiosulfate to cyanide in the detoxification process from cyanide and is able to insert sulfur atom in the iron–sulfur cluster. A study of the uniformly  $^{15}\text{N}$  isotopic labeling by high resolution NMR, before obtaining the backbone sequential assignment, has been carried out. The sulfur loaded and the sulfur discharged forms of the enzyme show very similar HSQC spectra with a good spectral dispersion. Few resonances show changes in chemical shift between the two forms. Relaxation parameters  $T_1$ ,  $T_2$  and  $^1\text{H}$ – $^{15}\text{N}$  NOE of all amide nitrogen atoms, as well as isotope exchange kinetics, show that the two forms exhibit the same global correlation time and hydrodynamic properties. In parallel, essential dynamics studies show that formation and discharging of catalytic cysteine persulfide group has no significant impact on the overall conformation of the protein. These results, taken together, give a clearcut answer to the question if the catalytic mechanism of the enzyme involves a change in the conformation and/or in the mutual orientation of the two domains. On the contrary these results clearly indicate that upon the catalytic mechanism the two domains of the protein behave as a unique fold.

© 2003 Elsevier B.V. All rights reserved.

**Keywords:** Rhodanese; Sulfurtransferase; Essential dynamics

## 1. Introduction

Proteins of the rhodanese family appear to be ubiquitous in all forms of life [1,2]. In vitro these enzymes catalyze the transfer of the outer sulfur atom from thiosulfate to cyanide. During catalysis the enzyme cycles between two catalytic intermediates, the free enzyme (E), and a sulfur-loaded enzyme (ES).

The catalytic residue is a cysteine, which by reaction with a donor molecule like thiosulfate, acquires an extra sulfur atom. The substrate is a molecule able to accept the sul-

fane sulfur. One such molecule is the cyanide ion, which is converted into thiocyanate. Although widely distributed, the physiological role of the sulfurtransferase enzymes has not been completely established. Previous works demonstrated that mammalian rhodanese (thiosulfate: cyanide sulfurtransferase, EC 2.8.1.1) can act as a sulfur insertase, and re-generate redox centers in Fe–S proteins [3,4]. The X-ray crystal structure of the bovine liver rhodanese (RhoBov) shows that the single polypeptide chain, consisting of 293 aminoacid residues, is folded into two domains that display a similar conformation with a  $\alpha/\beta$  topology [5]. Most of the studies regarding the structural determinants and selectivity in the mechanism of action of rhodanese were performed on RhoBov and the results were interpreted stressing the importance of protein flexibility. Both kinetic and CD studies

\* Corresponding author. Tel.: +39-06-72594446;

fax: +39-06-72594328.

E-mail address: paci@uniroma2.it (M. Paci).

have shown conformational changes between enzyme intermediates in solution, involving secondary structure transitions. Protein intrinsic fluorescence was also used to follow the conversion from ES to E [6]. The observed quenching of the intrinsic fluorescence of rhodanese upon binding of sulfur was also explained invoking a possible generalized conformational change in the enzyme induced by persulfide formation [7,8]. Previous studies by water NMR proton relaxation [9] and by  $^{35}\text{Cl}$  NMR relaxation studies [10] reported that significant changes in the exposure to solvent or to anion binding respectively has been observed for the two catalytic states ES and E. These results have been interpreted as due to an important interdomain reorientation(s) between the two structural domains of the enzyme upon the catalytic cycle [10].

The rhodanese from *Azotobacter vinelandii* (RhdA) is one of the prokaryotic recently expressed enzyme [11–13] whose three-dimensional structure has been elucidated [14]. Each domain displays a  $\alpha/\beta$  topology, with a central parallel five-stranded  $\beta$ -sheet surrounded by  $\alpha$ -helices on both sides. The catalytic functional site of rhodanese is due to the unique Cys residue 230 located close to the cleft between the two domains and all side chains essential for the catalysis are provided only by the second domain [14]. The conformation of the main chain around the active site is highly similar in RhdA with respect to RhoBov, although some residues in the active site are different. The amino acid sequence identity for these two enzymes is about 22%. More recently, soaking experiments performed on native RhdA crystals and subsequent crystallographic refinements gave the first insights into the sulfur-free form of this protein. It was observed that side chains of the catalytic Cys230 and Trp195 and Arg235 changed their orientations with respect to the ES form, but no other significant change in the overall conformation has been observed [14].

Special care has to be taken when deriving structural features of E and ES forms of rhodanese, as it was shown that interaction of the two states with anions such as thiocyanate and cyanide cause conformational transitions that inactivates the enzyme. Chow et al. [15] proposed a model in which the bovine free enzyme in the absence of a sulfur-donor substrate, slowly relaxes to a conformer outside the catalytic cycle. A partial irreversible inactivation was also observed after prolonged treatment with cyanide although no associated structural changes were reported [16]. Activity measurements on the RhdA protein showed that incubation of the native protein with either cyanide or sulfite lead to partial enzyme inactivation [14]. Prolonged incubation with excess of thiosulfate are needed to recover partially the rhodanese activity.

In the present study we report the results obtained by NMR spectroscopy of the two forms of rhodanese of *A. vinelandii* using uniformly  $^{15}\text{N}$ -labeled protein. H–N correlation spectra and  $^{15}\text{N}$  relaxation rates of the two forms, also in the absence of backbone assignments, were used to assess differences and similarities in the overall conformation and

to monitor possible differences in flexibility of ES and E. Characteristics such as chemical shift dispersion and line-shape can provide a first insight into the folding properties of the two forms of the protein in solution. The exquisite sensitivity of nitrogen chemical shift to variations of magnetic environment is a warranty that a reorientation of the two domains would imply a large difference in chemical shift of a significant number of backbone NHs between the two forms. The same would be true also for changes in the conformation or aggregation state of the protein in the presence of anions that can lead to inactive forms of the enzyme.  $^{15}\text{N}$  NMR relaxation times in the absence of backbone assignment can be used to study the overall hydrodynamic shape of the protein going from ES to E state. The overall results will be compared with molecular dynamics simulation studies performed on a sulfur charged and discharged forms.

## 2. Materials and methods

### 2.1. Expression of the uniformly labeled enzyme

Cell mass is predominately grown on unlabeled rich media allowing growth to high cell densities. Following growth in Luria–Bertani medium (LB), cells are exchanged into an isotopically defined minimal media at higher cell densities optimized for maximal protein expression. The protein was expressed in the *E. coli* BL21 pREP4 strain using the pQER1 plasmid and the antibiotics for the selection of *E. coli* transformants were used at the following concentration: 100  $\mu\text{g}/\text{ml}$  ampicillin, 25  $\mu\text{g}/\text{ml}$  kanamycin [13]. The general protocol for isotope labeling was as described by Marley et al. [17]. Cells were grown in 600 ml of LB at 37 °C shaken at 180 rpm. Upon reaching optical cell densities at 600 nm  $\sim 0.7$ , the cells were pelleted by a 25 min centrifugation at 5000 rpm. The gels were then washed and pelleted using an M9 salt solution (1 l of autoclaved 5XM9 salt: 15 g  $\text{KH}_2\text{PO}_4$ , 64 g  $\text{NaHPO}_4 \cdot 7\text{H}_2\text{O}$ , 2.5 g NaCl, 5 g  $\text{NH}_4\text{Cl}$ , pH 7.2). The cell pellet was resuspended in 400 ml of isotopically labeled minimal media (1 l of minimal media was composed by 200 ml of 5XM9 salts, 20 ml of D-glucose stock 20 g/100 ml, 10 ml basal vitamins Eagle Media, *Life Sciences Technology*, 2 ml of 1 M  $\text{MgSO}_4$ , 0.1 ml of 1 M  $\text{CaCl}_2$ ) and the protein expression was induced after 1 h by addition of isopropyl- $\beta$ -D-thiogalactoside (IPTG) to a concentration to a concentration of 1 mM. After a 4-h incubation period the cells were harvested. For isotope labeling the expression medium substituted of isotopically labeled  $^{15}\text{NH}_4\text{Cl}$  (99%). The incorporation rate for  $^{15}\text{N}$  was estimated by NMR to be  $\sim 90\%$ . Cell disruption was carried out by incubation with 0.6 mg/ml lysozyme 50 mM Tris–HCl, 0.3 M NaCl buffered at pH 7.5 and sonication. RhdA was purified by chromatography on Ni–NTA agarose column.

The His-tagged protein was eluted using 50 mM Tris–HCl buffer, pH 7.0, 0.3 M NaCl, 10% Glycerol, 0.2 M imidazole and precipitated in 75% saturated ammonium sulfate. The

protein concentration was determined using  $A_{280\text{nm}} = 1.3$  for 0.1% solution [12] and the molecular mass was 31 kDa. Rhodanese activity was measured by the discontinuous colorimetric assay described by Sörbo [18]. The presence of the His-tag did not affect enzymatic activity. The E form was prepared by adding a 10-fold molar excess of cyanide to ES rhodanese in 50 mM Tris–HCl buffer 0.3 M NaCl at pH 7.4, followed by a 10 min incubation at room temperature. Excess cyanide and thiocyanate were removed by using Centricon-3 (3000 MW cut-off, Amicon). For control the sulfur-loaded form, to which no cyanide was added, was analogously treated. The conversion of ES to E can be monitored by measuring the increase in the fluorescence quantum yield that accompanies the removal of the persulfide sulfur [19].

## 2.2. NMR spectroscopy

Sample of  $^{15}\text{N}$ -labeled RhdA and N-terminal domain of RhdA were prepared and concentrated to 0.2 mM in 50 mM Tris–HCl buffer at pH 7.2 and 0.3 M NaCl. Two-dimensional  $^{15}\text{N}$ – $^1\text{H}$  HSQC were measured at 20 °C on a Bruker Avance 700 MHz NMR spectrometer equipped with a  $z$ -gradient triple resonance probe. Instruments are part of the Joint Center for NMR of INFM (National Institute for Physics of Matter, the ISS (National Institute for Health, Italy) and the University of Rome Tor Vergata.

Data were processed and analyzed on IRIS O2 work station (Silicon Graphics) using NMRPipe [20] and NMRView [21].

$^{15}\text{N}$  relaxation experiments [22] were run as water flip-back versions. Six different time delays up to ca 1.5 T were used for  $T_1$  and  $T_2$  measurements, and the relaxation times were extracted through least-squares fitting of peak intensities.

The experiments of the exchange with  $\text{D}_2\text{O}$  were performed dissolving the freeze-dried uniformly  $^{15}\text{N}$ -labeled ES and E forms in  $\text{D}_2\text{O}$  buffer (50 mM Tris–HCl, pH 7.2, 0.3 M NaCl). The spectra  $^1\text{H}$ – $^{15}\text{N}$  correlation spectra were recorded after different times: 1, 2, 5, 12, 24 h and 7 days.

## 2.3. Molecular dynamics simulations

In order to characterize the local dynamics of the RhdA enzyme at molecular level, we performed three molecular dynamics simulations corresponding to the ES and the sulfur free enzyme in both the protonated (E) and deprotonated ( $\text{E}^-$ ) forms of the catalytic Cys230 residue. This choice is due to the possible ambiguity of the protonation state of the cysteine, considering the particular chemical environment present in the active site of RhdA. Moreover, classical molecular dynamics cannot reproduce bond forming or breaking events, thus two different simulations for the unloaded enzyme were needed.

The X-ray structure of ES was taken from the RCSB Protein Data Bank (code number 1e0c), which was solved by

Bordo et al. [14]. It was solvated by 9639 water molecules, including the crystallographic water and 10 sodium ions were added to ensure electric neutrality. The whole system was embedded in a rectangular box of 6.22, 7.07, 7.61 nm<sup>3</sup>, which gives an approximately normal density and the volume was kept fixed. Hence, an equilibration was realized by raising gently the temperature from 50 to 300 K during a simulation of 100 ps. This was followed by a long molecular dynamics simulation of 6.9 ns at constant temperature (300 K), which was used for the analysis. Second, starting from an equilibrated structure of the above system, taken after 4.4 ns, we performed two simulations, each of 4.0 ns-long, in which the Cys230 residue was modified according to the two sulfur free enzyme forms ( $\text{E}^-$  and E).

Note that all bonds were constrained to their own equilibrium values by means of the LINCS [23] algorithm. The simulations were conducted in periodic boundary conditions using a cut off radius of 1.0 and 1.5 nm for the van der Waals and the Coulomb interactions respectively. A time step of 2 fs was used and the Gaussian isothermal algorithm [24] was adopted to fix the temperature. All simulations were carried out with the GROMACS [25] simulation package using the GROMOS96 [26] force field.

## 3. Results and discussion

### 3.1. H–N correlation spectra

Fig. 1 shows the  $^1\text{H}$ – $^{15}\text{N}$  correlation experiments recorded with uniformly labeled samples of RhdA respectively in the two forms (ES and E). The correlation spectra of RhdA has an excellent dispersion and very good lineshape considering the relatively high MW of this protein (31 kDa). In fact there are only very few examples of monomeric proteins of this size amenable to the study in solution by NMR.

The large similarity between the spectra of ES and E allows to draw some preliminary conclusions also in the absence of the backbone sequence assignment. In fact the two spectra differ in the position of a small number of peak indicating that no significant change in conformation is involved. This observation was made in buffered solution and after treatment and dialysis of the excess of potassium cyanide, and hence in a different situation of the soaking experiments already performed to study this conformational transition [14]. ES can be readily converted into E by addition of potassium cyanide or viceversa thiosulfate and then dialyzing out the excess of reagent, as described in Section 2. The position of catalytic Cys230 has been univocally assigned in the two spectra by comparison with the chemical shift obtained with a selectively labeled sample (paper in preparation) (these resonances are indicated in Fig. 2). Fig. 3 shows the overall difference, using a single parameter to measure the chemical shift difference of the whole NH group [27]. Only few peaks (6 out of 250) show a  $\delta > 0.1$  ppm, one of which is Cys230 ( $\delta = 0.19$  ppm), and other 15 show  $0.1 >$

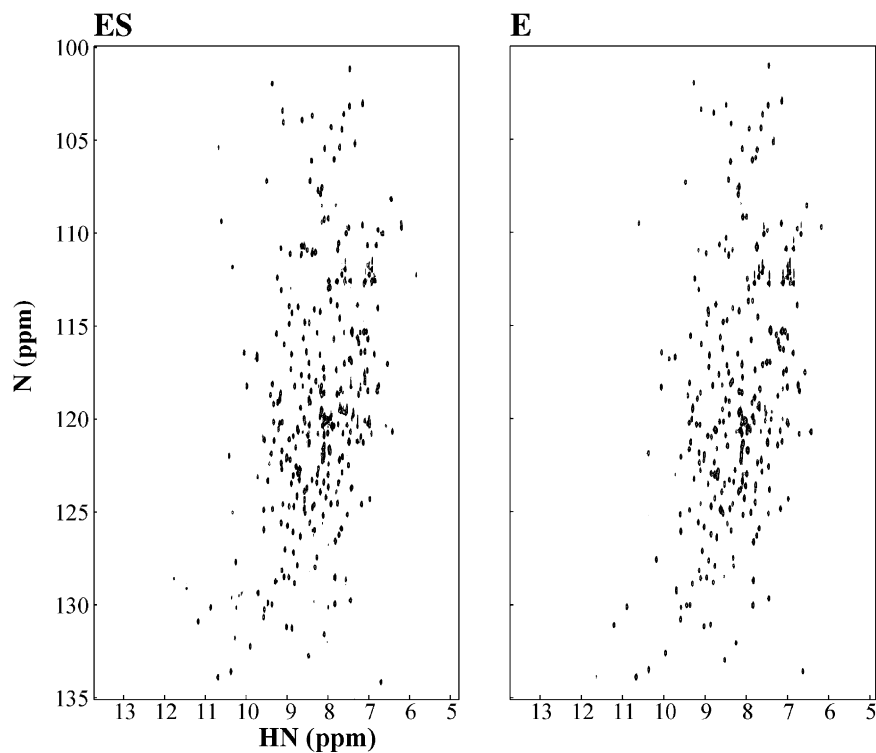


Fig. 1.  $^1\text{H}$ - $^{15}\text{N}$  HSQC correlation spectra of the of ES and E form of the 0.2 mM RhdA in 50 mM Tris-HCl buffer, pH 7.2, 0.3 M NaCl.

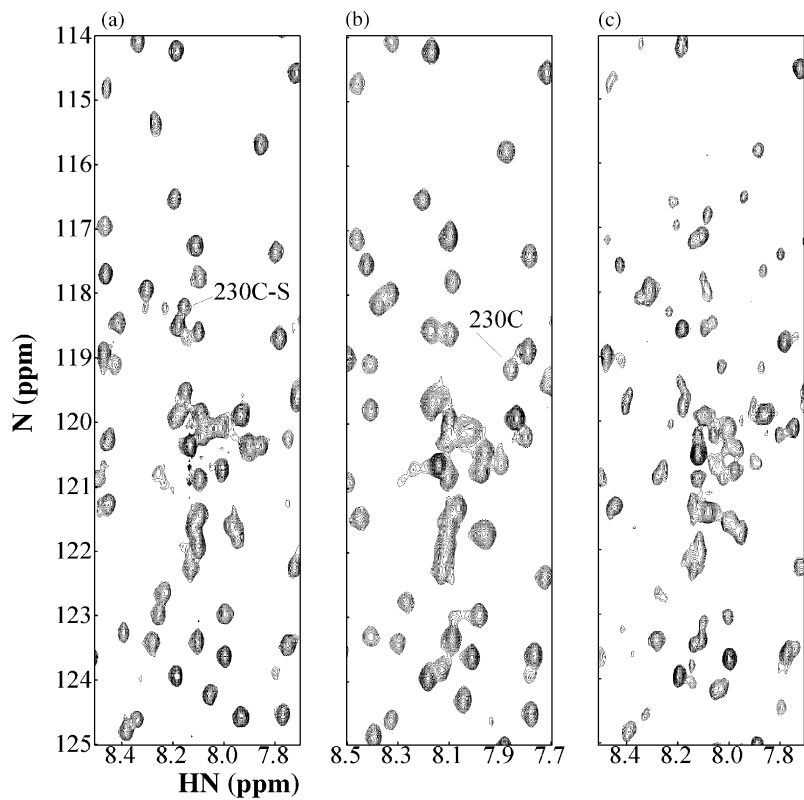


Fig. 2. Spectral regions of  $^1\text{H}$ - $^{15}\text{N}$  HSQC correlation spectra of the 0.2 mM RhdA  $^1\text{H}$ - $^{15}\text{N}$  HSQC spectrum of ES (a) and E form of RhdA (b); ES form in presence of thiosulfate and an excess of  $\text{CN}^-$  (c) (see text). The  $^1\text{H}$ - $^{15}\text{N}$  resonance of Cys230 in the ES and E forms is showed.

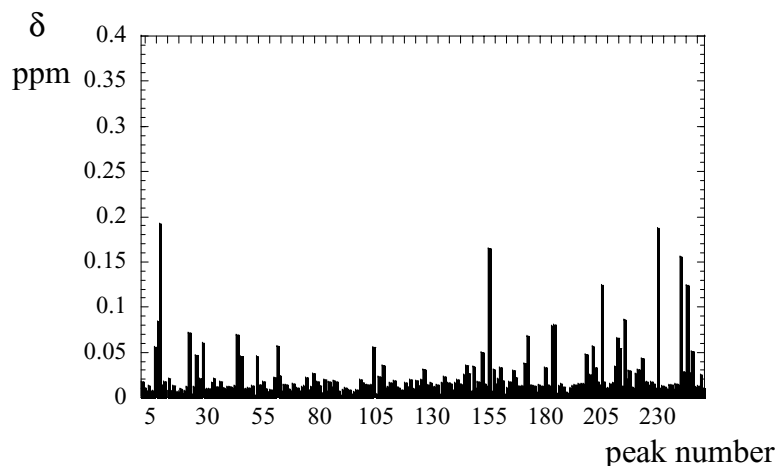


Fig. 3. H–N chemical shift differences ( $\delta$ ) between the ES and E forms of RhdA.  $\delta$  averages the effects on the H and  $^{15}\text{N}$  chemical shift and is defined as  $\delta = [(\Delta\delta_{\text{HN}}^2 + \Delta\delta_{\text{N}}^2/25)/2]^{1/2}$  [22].

$\delta > 0.5$  ppm. This indicates that only limited changes in the backbone conformation occur when converting the ES into the E form. Moreover, the number of aminoacids showing some difference in chemical shift is remarkably close to the expected conformational transition already calculated for RhoBov, for which a transition of 20 aminoacid from coil to  $\beta$ -sheet was hypothesized when going from the E to the ES forms [28]. However, as already stated above, bovine and *A. vinelandii* rhodaneses differ in the number of cysteines, the latter having a single cysteine residue.

A different situation was observed in the case when RhdA was first treated with thiocyanate and then, without dialyzing, an excess of cyanide was added to produce the E form. Fig. 2c shows the resulting H–N correlation spectrum. Two observations can be made: a large number of peaks show a significant decrease in intensity and new peaks are evident, corresponding neither to E nor to ES forms. A more detailed analysis reveals that peaks are closer to the position observed in the E form. This result indicates that, under these conditions, rhodanese is present in a significantly different state. The lower intensity observed for a number of peaks can be explained either by a conformational exchange between different conformations in the micro- to millisecond scale, partial aggregation of the protein, or a combination of both. This new aspect of the behavior of the protein will be studied in more detail in the future.

### 3.2. $^{15}\text{N}$ NMR relaxation measurements

To further characterize the possible differences between the two states of RhdA,  $^{15}\text{N}$   $T_1$  and  $T_2$  relaxation times, as well as steady-state  $^1\text{H}$ – $^{15}\text{N}$  NOEs were measured. As expected from the high similarity of chemical shifts observed, data obtained in the two cases are very similar and the results for the ES form are summarized in Table 1. The observed average values were  $\langle T_1 \rangle = 1.54$  s,  $\langle T_2 \rangle = 40.6$  ms. Using the  $T_1/T_2$  ratio approach [22], it was possible to calculate a

correlation time of 16.8 ns. Taking into account the temperature at which these measurements were performed (20 °C), this value is reasonable for a monomeric form of the enzyme (MW = 31.0 kDa). Very similar results were observed for the E form (data not shown). The measured values in the latter case were  $\langle T_1 \rangle = 1.50$  s,  $\langle T_2 \rangle = 40.2$  ms, yielding the same overall correlation time. This result indicates that there is no significant change in the overall conformation of the molecule and the global shape of the enzyme in the two forms remains unchanged.

In view of the fact that only 21 peaks over a total of 250 show some difference in chemical shift between the E and ES forms, changes in conformation are likely confined to a small region around the active site. Although we lack the assignment of the peaks in the  $^1\text{H}$ – $^{15}\text{N}$  correlation spectrum, these 21 peaks can be used as a sort of probe around the active site of the protein. The following question was if the changes in chemical shift observed for these peaks was also accompanied by a change in the relaxation parameters of the corresponding  $^{15}\text{N}$  backbone amide. Table 2 summarizes for most of these peaks the observed  $T_1$  and  $T_2$  relaxation times observed in the two enzymatic forms. From this result we can expect that the active site of the two forms shows a similar degree of flexibility.

Most of the residues of RhdA show no significant contribution of internal motions in the relaxation parameters of

Table 1  
Mean values of  $^{15}\text{N}$   $T_1$ ,  $T_2$  and NOE of the resonances of ES and E form of RhdA measured at 700 MHz

	ES <sup>a</sup>	E <sup>b</sup>
$\langle T_1 \rangle$ (s)	1.54 ± 0.21	1.5 ± 0.18
$\langle T_2 \rangle$ (s)	0.041 ± 0.010	0.40 ± 0.011
$\langle \tau_m \rangle$ (ns)	16.8 ± 08	16.8 ± 0.7

Data of  $T_1$  and  $T_2$  measurements were fitted as a single exponential.

<sup>a</sup> 203 peaks average.

<sup>b</sup> 193 peaks average.

Table 2

Measured  $T_1$  and  $T_2$  relaxation times for  $^{15}\text{N}$  backbone amide of the 19 resonances showing a change in chemical shift in the two forms (E and ES) of RhdA

Peak	E		ES	
	$T_1$ (s)	$T_2$ (ms)	$T_1$ (s)	$T_2$ (ms)
6	1.73	36.8	1.71	34.9
7	1.55	35.4	1.66	35.7
8	1.63	39.4	1.71	39.9
11	1.39	36.1	nd <sup>a</sup>	nd
21	1.81	37.6	1.74	40.1
27	1.70	nd	1.76	39.5
42	1.98	49.6	1.92	49.1
44	1.64	36.3	1.66	37.7
48	1.36	nd	1.46	nd
51	1.59	41.7	1.66	39.4
134	1.65	42.3	1.62	47.8
144	2.20	45.6	2.17	43.5
148	1.42	43.6	1.47	46.5
182	1.64	37.1	1.70	36.8
183	1.58	43.1	1.72	45.9
200	1.32	50.0	1.32	53.3
204	1.51	nd	1.40	nd
229	1.64	38.9	nd	nd
238	1.78	nd	1.79	nd

<sup>a</sup> nd: not determined.

$^{15}\text{N}$ , as can be deduced from the fact that only 18 out of 242 peaks showed  $^1\text{H}$ - $^{15}\text{N}$  NOE less than 0.6. Up to now we have not identified the specific residues but it is interesting to note that a comparable number of residues appears flexible in the molecular dynamics simulation. Thermodynamic calculations performed by Wang and Volini [29] estimated a difference of 8 kcal/mol between the ES and E forms of RhoBov and suggested that the change is consistent with the interconversion of about 20 aminoacidic residues from ordered secondary structure to a disordered coil type structure [28]. Although we found also a very similar number of residues showing a difference in chemical shifts between the two forms, the almost identical relaxation parameters of the corresponding amide  $^{15}\text{N}$  are not compatible with a transition to a more flexible coil structure going from the ES to the E form.

### 3.3. Solvent accessibility studies

A second study has been performed regarding the solvent accessibility of the active site in the two forms. To measure this property, we have recorded  $^1\text{H}$ - $^{15}\text{N}$  correlation spectra at different times after dissolving the protein in  $\text{D}_2\text{O}$ , and following the intensities of the cross-peaks. In each form of the enzyme about 115 peaks show a high rate of exchange with  $\text{D}_2\text{O}$ , in fact they disappear immediately when the protein is dissolved in  $\text{D}_2\text{O}$ . On the contrary about 94 peaks seem to have a very slow rate of exchange with  $\text{D}_2\text{O}$ , as they are visible even after 1 week.

In particular, there are 15 peaks that show a different rate of exchange with  $\text{D}_2\text{O}$  in the two forms, 10 peaks of these

showing a higher rate in the E form with respect to the ES form. Two peaks among these peaks show different chemical shifts in the E and ES forms. Fig. 4 shows a selected region of the  $^1\text{H}$ - $^{15}\text{N}$  HSQC spectra of the ES and E form and the observed intensity variation at different time of  $\text{D}_2\text{O}$  exposure. This result points out that the solvent accessibility does not show large differences between the two forms, indicating that no substantial changes in the solvent exposure of the molecule occur when the enzyme goes from ES to E form. In particular the rate of exchange with  $\text{D}_2\text{O}$  of some peaks of the E form is higher than that observed in the ES forms. An analysis of the crystallographic structure of RhdA in the ES form shows that about 90 amide groups of the backbone could be accessible to the solvent. This result seems to be in agreement with observations made for the bovine enzyme, indicating an enhanced solvent accessibility in the unloaded form [9,10]. This effect could be explained only as the consequence of rearrangements of some side chains of the active site residues, leading to a more open channel that facilitates the interaction with small ions, as thiosulfate.

### 3.4. Molecular dynamics simulation

Molecular dynamics was used to elucidate the overall dynamical behavior as well as the local rearrangement in the active site of RhdA during its catalytic cycle. As reported in Section 2 the simulations have been made for the ES form, for E one, and for the deprotonated Cys230 ( $\text{E}^-$  form) respectively. All the analysis were performed on the last 3.0 ns of the three simulated trajectories, which are shown to be the most equilibrated and stable parts. Results are depicted in Fig. 5a and b, where the root-mean-square (RMS) deviations and fluctuations per residue are reported. Remarkably, the same agreement is encountered when the main collective motions are examined by means of essential dynamics (ED) analysis [30].

In fact this procedure, based on the diagonalization of the covariance matrix of the atomic positional fluctuations, gives collective intramolecular motions which can be ordered according to the corresponding amplitudes (i.e. the eigenvalues). In this way the configurational subspace where most of the conformational fluctuations are present can be detected and characterized.

A comparison of the first 15 eigenvalues, calculated on  $\text{C}^\alpha$  coordinates has been performed. The ES and E forms are very similar and they show an overall enhanced flexibility with respect to the  $\text{E}^-$  form (data not shown). The local dynamics of the active site was also studied. Atom displacements of residues 230–236 (data not shown), which form the active site, relative to the first eigenvector also indicates a close correspondence in the dynamics of the ES and E forms of RhdA.

Moreover, regions between residues 119–144 and 54–62 (in red in Fig. 5c) show high RMS fluctuation which correspond, in the X-ray crystal structure, to the tether between the two domains and a loop respectively. In Fig. 5b it is pos-

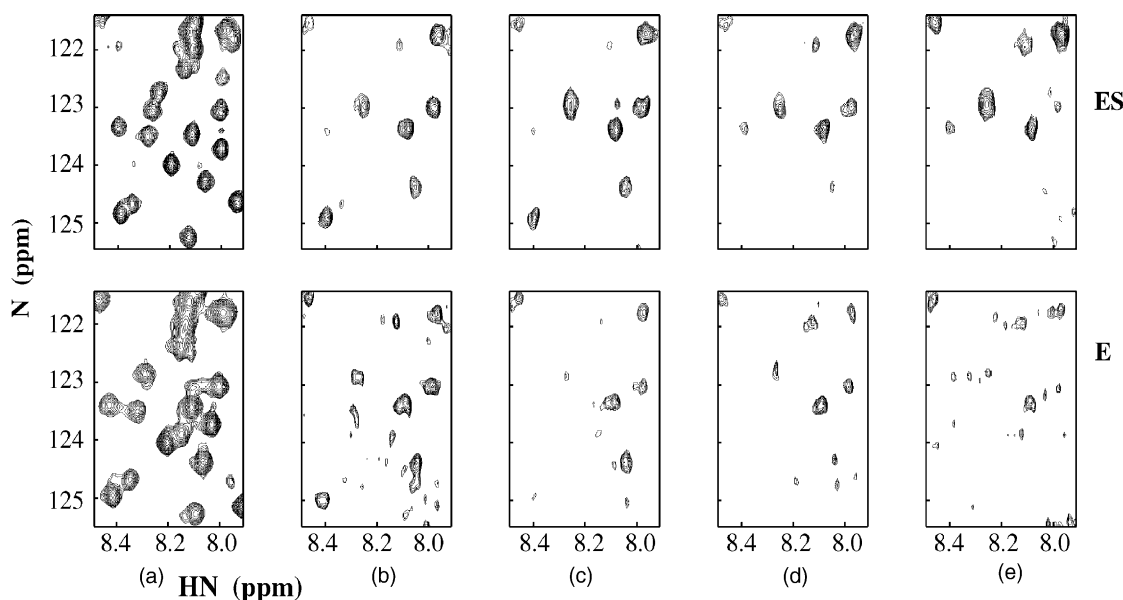


Fig. 4. Solvent accessibility of the two forms of the RhdA measured by the deuterium exchange of NH labile protons. Selected region of  $^1\text{H}$ - $^{15}\text{N}$  HSQC spectra of ES (upper row) and E (lower row) forms (a) RhdA 0.2 mM in  $\text{H}_2\text{O}$  (50 mM Tris-HCl, pH 7.2, 0.3 M NaCl) and in  $\text{D}_2\text{O}$  at different times: (b) 1 h, (c) 2 h, (d) 5 h, and (e) 7 days after exposure.

sible to distinguish two regions, comprising residues 92–105 and 234–246, that show the lowest RMS fluctuation. These regions correspond to the two helices (helix 6 and helix 13 in the crystal structure, in green in Fig. 5c) that are located in the contact face between the domains.

Overall from ED only local slight differences were observed between the ES and E forms with respect to their dynamical behavior, leaving the overall shape unchanged with the absence of motions between the two domains. They correspond to regions including residues 31–40, 119–128, and 154–162 (in blue in the Fig. 5c). In particular, the ES form seems to be more flexible than the E form except for the region between residues 31–40. In the bovine rhodanese, it was shown that mutation of Cys254 produced an E form that was readily digested with trypsin and subtilisin, whereas the wild type or the mutated ES were not [31–34]. This result was interpreted by means of a destabilization of the D'  $\alpha$ -helix produced by the mutation in E but not in ES, generating structural flexibility in the active site of E to permit proteolytic digestion [31]. The different number of cysteines, and the lack of formation of different disulfide bridges involving the catalytic Cys230 in RhdA when compared with RhoBov can play a role in this different behavior. RhdA lacks of other cysteines apart from the catalytic one and shows a glycine Gly237 instead of Cys254. In any case, it shows a high conformational stability. This fact can lead to the conclusion that in RhdA, the stability of the helix 13, is attained by a series of interactions different from those occurring in RhoBov (D'  $\alpha$ -helix or helix 11), without the need of a second cysteine to yield this effect. In fact, a careful analysis of the tertiary structure of RhdA shows that there are three H-bonds between the helix 6 and helix 13 (97–233, 90–234, 103–240)

and hydrophobic interactions, such as the side chains interactions between Trp100-His233 and Trp9-His234 that induce a conformational stability of the interdomain region. On the other hand, the three-dimensional structure of RhoBov shows only one H-bond (Arg110-Gly250) between the two helices in the catalytic site, whilst hydrophobic interactions seem to play a more significant role. Particularly, the electronic-interaction between the  $\text{S}_\gamma$  of Cys254 and the indole of the Trp113, as already observed for other S-aromatic interactions [35], could be important for the conformational stability and for explaining the major flexibility observed in the mutant C254S of RhoBov. Furthermore, bovine and *A. vinelandii* enzymes have distinct aminoacid composition around the conserved catalytic cysteine and two loops (33–42 and 189–201 residues), located next to the catalytic loop of RhoBov, are eight and four residues shorter in RhdA [14]. Thus the two enzymes could display a different flexibility and change in protein surface shape in the vicinity of the catalytic center.

Recently it was found that the replacement of Thr232 with Ala in the active site of RhdA increased its sulfur-transfer activity [36]. Conversely, the corresponding mutation in the bovine enzyme (Lys249 mutated in Ala) inactivated the enzyme [16]. So in RhdA the electrostatic interactions, which are the driving force for the binding of anions (cyanide, thiosulfate, etc.) in the sulfur-transfer activity, seems to be not altered by substitution of Thr232. Moreover, the use of thiosulfate during the purification steps was not required for RhdA, as it was for the bovine enzyme [37], since its E form was very sensitive to the oxidative reactions [38]. In addition, the functional stability of *A. vinelandii* rhodanese was not affected by the presence of thiosulfate and the protein

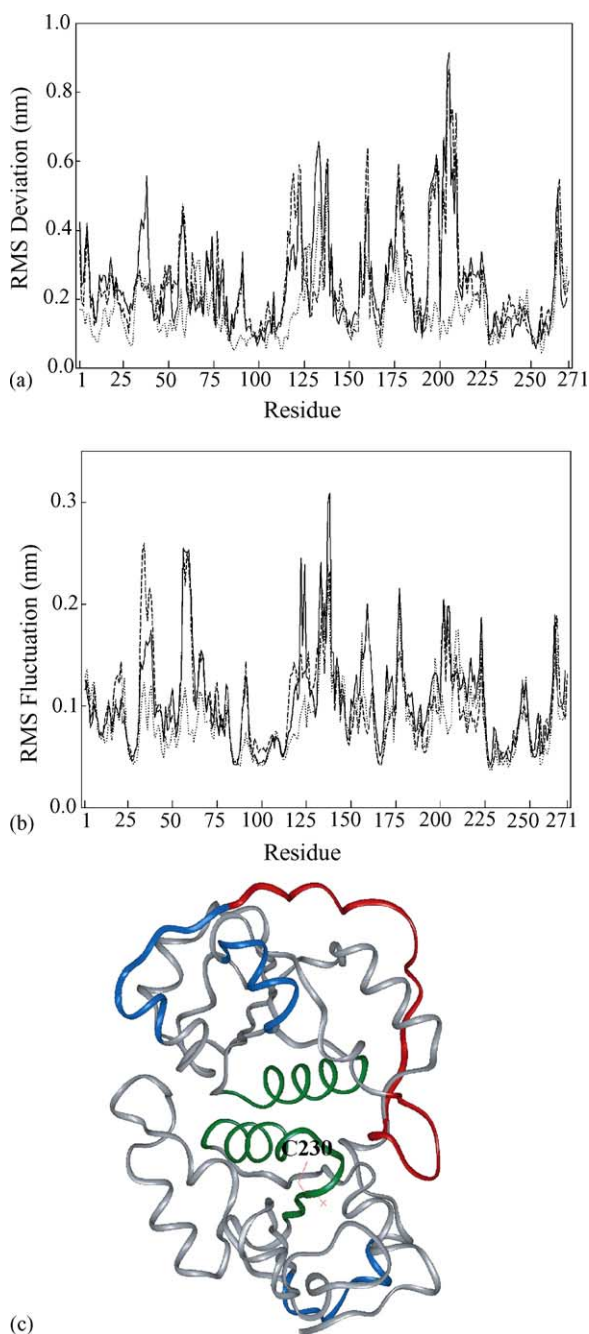


Fig. 5. Molecular dynamics simulation of RhdA: (a) RMS deviation per residue, calculated on C<sup>α</sup> atom coordinates (ES solid line, E<sup>-</sup> dotted line and E dashed line); (b) RMS fluctuation per residue, calculated on C<sup>α</sup> atom coordinates (ES solid line, E dashed line and E<sup>-</sup> dotted line); (c) ribbon representation of crystal structure of RhdA. In (c) the regions between residues 119–144 and 54–62 with high RMS fluctuations are shown in red; the helix 6 and 13, that show the smallest RMS fluctuations, are represented in green and the regions including residues 31–40, 119–128, and 154–162, that show differences between the ES and E forms with respect to their dynamical behavior, are represented in blue.

appeared to be more stable compared to the bovine enzyme [36]. These results may be interpreted as evidence of differences in the catalytic properties of RhdA compared with those of vertebrate rhodanese.

#### 4. Conclusions

A full model of the rhodanese catalytic mechanism is still unavailable. Based on many different observations, it is generally accepted that the enzyme undergoes conformational changes when passing from one state to the other within the catalytic cycle. In the mid-1980s the accepted picture of the catalytic cycle of rhodanese pointed out that the architecture of rhodanese was particularly adapted for motion [39]. We have investigated the structural properties of the two forms of the *A. vinelandii* rhodanese by <sup>15</sup>N NMR relaxation on the uniformly <sup>15</sup>N-labeled protein and by deuterium exchange and compared these results with those obtained by molecular simulations and essential dynamics. No change in the overall shape of the enzyme was observed and thus change of the relative orientation between the two domains can be excluded going from ES to the E state. Moreover, significant differences were not observed in the backbone conformation and flexibility between the two forms. This result gives for RhdA a clearcut answer to the question if the catalytic mechanism of the enzyme involves a mutual conformational change of the contact region between the two domains indicating that the protein behave as an unique fold. The role of the tether is just to connect the two domains with no functional utility. Only small rearrangements, likely confined around the active site, seem to be the only differences between ES and E. The complete sequential assignment will yield a comprehensive picture of the local flexibility and will be very valuable for the interpretation of the enzymatic mechanism.

The low sequence identity of the RhdA with the eukaryotic rhodanese, the different functional stability and flexibility with the bovine rhodanese, as suggested by the present work and others [36], may propose that the two enzymes share common functions but may also be used differently by prokaryotic and eukaryotic organisms.

#### Acknowledgements

The technical assistance of Fabio Bertocchi is gratefully acknowledged. This research was supported by MURST PRIN project “Solfotransferasi procariotiche” (1999–2001 and 2002–2003) and the target Project of Italian CNR “Biotecnologie”. The Italian FIRB of MIUR is gratefully acknowledged for funding.

#### References

- [1] Westley J. Rhodanese and the sulfane pool. In: Jakoby WB, editor. The enzymatic basis of detoxification. New York: Academic Press; 1980. p. 245–61.
- [2] Ray WK, Zeng G, Potters MB, Mansuri AM, Larson TJ. J Bacteriol 2000;182:2277–84.
- [3] Finazzi Agrò A, Mavelli I, Cannella C, Federici G. Biochem Biophys Res Commun 1976;68:553–60.

- [4] Pagani S, Eldridge M, Eady R. *Biochem J* 1987;244:488.
- [5] Ploegman JH, Drent G, Kalk KH, Hol WG, Heinrikson RL, KeimWeng PL, et al. *Nature* 1978;273:124–9.
- [6] Davidson B, Westley J. *J Biol Chem* 1965;240:4463–9.
- [7] Finazzi Agrò A, Federici G, Cannella C, Cavallini D. *Eur J Biochem* 1972;28:89–93.
- [8] Guido K, Horowitz PM. *Biochem Biophys Res Commun* 1975;67:670–6.
- [9] Blicharska B, Koloczek H, Wasylewski Z. *Biochim Biophys Acta* 1982;708:326–9.
- [10] Man M, Bryant RG. *J Biol Chem* 1974;249:1109–12.
- [11] Pagani S, Sessa G, Sessa F, Colnaghi R. *Mol Biol Int* 1993;29:595–604.
- [12] Pagani S, Franchi E, Colnaghi R, Kennedy C. *FEBS Lett* 1991;278:151–4.
- [13] Colnaghi R, Pagani S, Kennedy C, Drummond M. *Eur J Biochem* 1996;236:240–8.
- [14] Bordo D, Deriu D, Colnaghi R, Carpen A, Pagani S, Bolognesi M. *J Mol Biol* 2000;298:691–704.
- [15] Chow SF, Horowitz PM, Westley J, Jarabak Jr. *J Biol Chem* 1985;260:2763–70.
- [16] Luo GX, Horowitz PM. *J Biol Chem* 1994;269:8220–5.
- [17] Marley J, Lu M, Bracken C. *J Biomol NMR* 2001;20:71–7.
- [18] Sörbo B. *Rhodanese Acta Chem Scand* 1953;7:1123–30.
- [19] Horowitz P, Criscimagna NL. *J Biol Chem* 1983;258:7894–6.
- [20] Delaglio F, Grzesiek S, Vuister GW, Zhu G, Pfeifer J, Bax A. *J Biomol NMR* 1995;6:277–93.
- [21] Johnson B, Blevins J. *J Biomol NMR* 1994;4:603–14.
- [22] Farrow N, Muhandiram DR, Singer AU, Pascal SM, Kay CM, Gish G, et al. *Biochemistry* 1994;33:5984–6003.
- [23] Hess B, Bekker H, Berendsen HJC, Fraije JGEM. *J Comput Chem* 1997;18:1463.
- [24] Allen MP, Tildesly DJ. *Computer simulation of liquids*. Oxford: Oxford University Press; 1987.
- [25] Van der Spoel D, Berendsen HJC, Van Buuren, AR, Apol E, Meulenhoff PJ, Sijbers ALTM, Van Drunen R. *GROMACS user manual version 3.0*. Nijenborgh 4, 9747 AG Groningen, The Netherlands. Internet: <http://www.gromacs.org>, 2001.
- [26] Van Gunsteren WF, Billeter S, Eising A, Hünenberger P, Krüger P, Mark A, Scott W. *Tironi biomolecular simulation: the GROMOS96 manual and user guide*. Biomos B.V., Hochschulverlag, 1996.
- [27] Grzesiek S, Stahl SJ, Wingfield PT, Bax A. *Biochemistry* 1996;35:10256–61.
- [28] Volini M, Wang SF. *J Biol Chem* 1973;248:7386–91.
- [29] Wang SF, Volini M. *J Biol Chem* 1973;248:7376–85.
- [30] Amadei A, Linssen BM, Berendsen HJC. *Proteins* 1993;17:412–25.
- [31] Islam TA, Miller-Martini DM, Horowitz PM. *J Biol Chem* 1994;269:7903–13.
- [32] Horowitz PM, Xu R. *J Biol Chem* 1992;267:19464–9.
- [33] Trumpower BL, Katki A, Horowitz PM. *Biochem Biophys Res Commun* 1974;57:523–8.
- [34] Shibantani T, Kramer G, Hardesty B, Horowitz PM. *J Biol Chem* 1999;274:33795–9.
- [35] Viguera AR, Serrano L. *Biochemistry* 1995;34:8771–9.
- [36] Pagani S, Forlani F, Carpen A, Bordo D, Colnaghi R. *FEBS Lett* 2000;23(611):1–5.
- [37] Horowitz PM, De Toma F. *J Biol Chem* 1970;245:984–5.
- [38] Horowitz PM, Bowman S. *J Biol Chem* 1987;262:14544–8.
- [39] Ploegman JH, Drent G, Kalk KH, Hol WGJ. *J Mol Biol* 1978;123:557–94.